



Nearshore Tsunami amplitudes across the Maldives archipelago due to worst case seismic scenarios in the Indian Ocean

Shuaib Rasheed¹, Simon C. Warder¹, Yves Plancherel¹, and Matthew D. Piggott¹

¹Department of Earth Science and Engineering, Imperial College London, UK

Correspondence: Shuaib Rasheed (s.rasheed18@imperial.ac.uk)

Abstract.

The Maldives face the threat of tsunamis from a multitude of sources. However, the limited availability of critical data, such as bathymetry (a recurrent problem for many island nations), has meant that the impact of these threats has not been studied at an island scale. Studies of tsunami propagation at the island scale but across multiple Atolls is also a challenging task due to the large domain and high resolution required for modelling. Here we use a high resolution bathymetry dataset of the Maldives archipelago, and corresponding high numerical model resolution, to carry out a scenario-based tsunami hazard assessment for the entire Maldives archipelago to investigate the potential impact of plausible far-field tsunamis across the Indian Ocean at the island scale. The results indicate that the bathymetry of the Atolls, which are characterized by very steep boundaries offshore, is extremely efficient in absorbing and redirecting incoming tsunami waves. Results also highlight the importance that local effects have in modulating tsunami amplitude nearshore, including the location of the Atoll in question, the location of a given island within the Atoll, and the distance of that island to the reef, as well as a variety of other factors. We also find that the refraction and diffraction of tsunami waves within individual Atolls contribute to the maximum tsunami amplitude patterns observed across the islands in the Atolls. The findings from this study contribute to a better understanding of tsunamis across complex Atoll systems, and will help decision and policy makers in the Maldives assess the potential impact of tsunamis across individual islands. An online tool is provided which presents users with a simple interface allowing the wider community to browse the simulation results presented here and assess the potential impact of tsunamis at the local scale.

1 Introduction

The 2004 Boxing day tsunami is the single most significant natural disaster to hit the Maldives in nearly a millennium of recorded history. The widespread impact of the tsunami, the loss of human life and the economic impact of the event is unprecedented in the history of the country, with losses estimated at over 62% of the Gross Domestic Product (GDP), representing the highest relative losses of any affected country (World Bank and System, 2005). The severity of the aftermath highlighted the necessity of developing a better understanding of tsunami propagation in the Indian Ocean (Okal and Synolakis, 2008). Field studies aiming to quantify the amplitudes and inundation levels of the 2004 Boxing Day tsunami across the Maldives revealed that different regions of the Maldives experienced vastly different levels of damage in spite of them having similar



25 elevation. These data imply that the amplitude and inundation levels across the Maldives depend strongly on the geography of
the islands and possibly on the source location of the tsunami (e.g., Fritz et al., 2006; Kan et al., 2007; Fujima et al., 2006).

Historical impacts of tsunamis are not well documented, and since large tsunamis occur with return periods in the hundreds of
years and affect very large scales, data from such events have rarely been recorded since oceanic observations began (Synolakis
and Bernard, 2006). As indicated by RMSI (2006), even though there is no documented historical record of a tsunami in the
30 Maldives prior to the December 2004 event, despite a written history spanning nearly a millennia, it is highly probable that
historical tsunamis generated from mega-thrust earthquakes in the Indian ocean have impacted the Maldives. Along this line,
Kench et al. (2006) also argue that the Maldives have been exposed to multiple tsunamis during the Holocene but it is not
possible to identify tsunami events from stratigraphic records due to the extremely dynamic geomorphology of coral islands.
Other flooding events known to impact the Maldives, for example those due to the periodic swells originating in the Southern
35 Ocean impacting the South and Central regions of the Maldives, and meteo-tsunamis in the form of local swells (Wadey et al.,
2017) are also not well-documented nor well-understood.

It is essential to understand the impact of potential tsunami events across the country at the island-scale to realize the
effectiveness of safety measures, embodied by the “safe island concept” in the Maldives (Naseer et al., 2006), and to evaluate
protective mitigation measures. High resolution numerical simulations are necessary to fully understand the impact of potential
40 tsunamis in the Maldives. Particular geographic features of the Maldives archipelago, through their role in modulating complex
wave reflection and refraction patterns, have likely resulted in some regions being impacted less and others being impacted
more. The ability to understand how local geography affects tsunami propagation within the archipelago represents a step
change in disaster risk management for the Maldives. However, accurate island scale tsunami simulations across the Maldives
have not yet been carried out because, until recently, bathymetry data of suitable resolution were lacking. Here we employ
45 a new bathymetry product built specially for the Maldives (Rasheed et al., 2020). This product represents an amalgamation
of new satellite-derived bathymetry ground-truthed with field data gathered over the past century (e.g., Gardiner, 1902, 1903;
Sewell, 1936; Hass, 1965; Stoddart, 1966). This new product enables high resolution ocean modelling across the archipelago,
and is used here to simulate, for the first time, the nearshore impacts of an array of plausible seismic scenarios in the Indian
Ocean on the Maldives.

50 Tsunami propagation has been modelled at single island scale (e.g. Tonini et al. (2014) in the Seychelles and Gelfenbaum
et al. (2011); Dilmen et al. (2018) in Tutuila, American Samoa), at single Atoll scale (e.g. Gica (2015) considered Midway
Atoll) and at large basin scales (as used in tsunami warning systems). However, hydrodynamic simulations of tsunami propaga-
tion across and within large complex Atoll systems, where local reflection and refraction patterns are simulated with sufficient
resolution to account for local effects, is rare. Even where hydrodynamic simulations of such domains have been carried out,
55 e.g. for Tokelau in the South Pacific (Orpin et al., 2016), complex multi-Atoll interactions have not been considered. The
Maldives archipelago, consisting of a string of multiple Atolls, each characterized by many islands and bathymetric features,
provides an excellent case study to assess tsunami propagation in a complex multi-Atoll system and learn how across-Atoll
and within-Atoll effects can influence the local impact of tsunamis.



Below we develop and discuss tsunami simulations for the Maldives designed to investigate the main factors that influence local variability in the maximum tsunami amplitudes across the islands. The analysis uses the better observed 2004 Boxing Day tsunami to validate the model. The model is then run accounting for various plausible far-field tsunami scenarios originating from around the Indian Ocean.

2 Methodology

2.1 Geological Setting

The Maldives archipelago stretches for approximately 900 km from North to South, and lies in the central region of the Chagos-Laccadive ridge, located in the central Indian ocean. The archipelago consists of 25 geographic Atolls, further classified as 16 complex Atolls, five oceanic faros and four oceanic platform reefs (Naseer and Hatcher, 2004). The Maldives archipelago contains the worlds largest Atoll system, with numerous reefs numbering in excess of 2000, representing 5% of the world's coral reefs (Emerton et al., 2009). Even though there are more than 1200 individual islands in the archipelago, the islands are very small, with the largest, Gan island in Hadhunmathi Atoll, being only 5 km² in size. The islands are extremely flat, with their topography rarely exceeding an elevation of 2 m above mean sea level (ADB, 2020). Approximately 200 of the islands are inhabited and numerous others are utilized for other purposes, especially for the tourism industry and the development of luxury resorts. Limited usable exposed land, rapid population growth in the past few decades and competition for land use, have led to a state of scarcity such that land reclamation is now taking place across the archipelago on an industrial scale (Duvat and Magnan, 2019). Studies indicate that the coastline of nearly all inhabited islands of the Maldives have been modified in the past few decades to cater for this growth (ADB, 2020). This in turn has an impact on the flow regime of the Atolls (Rasheed et al., 2021, 2020).

While it has been hypothesised that the complex bathymetry of the archipelago, shown in Figure 1(b), contributed to attenuated tsunami amplitudes across the archipelago (Fritz et al., 2006), a quantitative test of this hypothesis has never been attempted. As can be seen in Figure 1, one of the most prominent bathymetric features is the steep depth gradient characterising the Atolls and the lagoons, giving rise to the 'leaky bucket' concept that is used to describe flow in and out of the Atoll systems (Betzler et al., 2016).

The Northern Atolls of the Maldives are generally characterized by few exposed islands, separated by numerous channels with depths of about 30 m, with small individual reefs hosting islands (Riyaz and Suppasri, 2016). The Southern Atolls tend to be more continuous, comprising of large shallow lagoons with multiple islands and fewer deep channels. Most large islands of the Maldives have developed on the rims of the Atolls, with the central lagoon of most Atolls devoid of any large islands (Luthfee, 1995).

Towards the open ocean, the bathymetry rapidly drops from just below sea level to more than 1000 m within 1 km from the Atoll rim. Even towards the Atoll basins where the depths are much more shallower, this steepness is evident in bathymetry charts. The bathymetry of the channels between the Atolls varies across the archipelago; in the Maldives inner sea, which separates the double chain of Atolls in the central regions of the archipelago running north to south, the bathymetry varies from



300 m to more than 500 m, gradually deepening towards the south east. In the Southern region, the depths of the channels between the Atolls are in excess of 1000 m (Luthfee, 1995).

2.2 Seismic scenarios

95 To build confidence in the model, we initially consider the 2004 event for validation against observational data. We employ the fault mechanism defined by Grilli et al. (2007), which discretizes the fault mechanism into five fault plates, as the primary tsunami-generating mechanism. Poisson et al. (2011) studied the event using various source models in numerical simulations with nested models of Sri Lanka and concluded that the fault model described by Grilli et al. (2007) is adequate for hydrodynamic modelling. This mechanism has also been used by a number of other studies to model the impact of the 2004 Boxing
100 Day tsunami across the Indian Ocean, e.g. in the Seychelles (Tonini et al., 2014).

To test the sensitivity of our results to the tsunami source model, we also employ here a multi-dimensional seismic scenario of the Boxing Day even, as defined by Tanioka et al. (2006), in addition to the simple fault model described by Grilli et al. (2007). The more complex model involves 12 fault plates in the spatial domain and also includes a temporal discretization of each fault plate. Harig et al. (2008) also used the more complex fault model identified in Tanioka et al. (2006) to study
105 the nearshore impacts in Indonesia and obtained results comparable to field data. By simulating two fault models, we can evaluate the impact of the fault model on the simulated tsunami. These two scenarios are labelled A (the 5-subfault case (Grilli et al., 2007)) and B (the 12-subfault case (Tanioka et al., 2006)). The parameters for each subfault for these two scenarios are summarised in Table 1.

Further, Okal and Synolakis (2008) identified 11 worst case seismic scenarios across the Indian Ocean which are capable of
110 generating transoceanic tsunamis, akin to the 2004 boxing day event. They carried out tsunami simulations for these scenarios, assessing the large-scale impact across the Indian Ocean. Wijetunge (2012) used these seismic scenarios to assess the resulting tsunami amplitudes at higher resolution along the coast of Sri Lanka. Here we consider eight selected scenarios (out of the 11 available from Okal and Synolakis (2008), summarised in Table 1), to assess the potential impact of some of the worst most-likely tsunamis that could affect the Maldives and to assess the role of across-Atoll and within-Atoll effects. The parameters
115 for these eight scenarios are summarised in Table 2, categorized according to the region of origin.

1. South Sumatra Subduction Zone

Studies such as RMSI (2006), which provide return periods for various hazards associated with the Maldives, predict return periods of approximately 140 years for tsunamis with amplitudes greater than 2 m in the Maldives that originate from the South Sumatra subduction zone. Given this relatively short return period, we consider all four plausible
120 worst-case scenarios from Okal and Synolakis (2008), as summarised in Table 2, with probable impact in the Maldives. Scenario 1 represents a repeat of the 24 November 1833 earthquake, which is reported to have generated a small tsunami observed as far west as the Seychelles. Scenario 2 represents the plausible worst-case scenario for the 1833 earthquake with the same focal geometry, but with an extended fault length of 900 km and increased slip of up to 15 m, releasing a total moment equivalent to the 26th December 2004 megathrust event. Scenarios 1a and 2a are modifications of scenar-



| Scenario | M_0 (dyn X cm) | Φ (deg) | δ (deg) | λ (deg) | L (km) | W (km) | h (km) | ΔU (m) | Source Center | | t (min) |
|----------|----------------------|-----------------|-------------------|--------------------|-------------|-------------|-------------|-------------------|----------------|-----------------|------------|
| | | | | | | | | | Latitude (deg) | Longitude (deg) | |
| A | 7.6×10^{30} | 323 | 12 | 90 | 220 | 130 | 25 | 18 | 94.57 | 3.83 | |
| | | 348 | 12 | 90 | 150 | 130 | 25 | 23 | 93.90 | 5.22 | |
| | | 338 | 12 | 90 | 390 | 120 | 25 | 12 | 93.21 | 7.41 | |
| | | 356 | 12 | 90 | 150 | 95 | 25 | 12 | 92.60 | 9.70 | |
| | | 10 | 12 | 90 | 350 | 95 | 25 | 12 | 92.87 | 11.70 | |
| B | 7.2×10^{22} | 340 | 10 | 90 | 100 | 100 | 10 | 26.1 | 94.57 | 3.83 | 0 |
| | | 340 | 10 | 90 | 160 | 100 | 10 | 0.0 | 95.55 | 2.37 | 1 |
| | | 340 | 10 | 90 | 150 | 90 | 10 | 29.6 | 95.23 | 3.23 | 1 |
| | | 340 | 10 | 90 | 150 | 100 | 10 | 7.3 | 94.25 | 4.45 | 3 |
| | | 340 | 10 | 90 | 150 | 100 | 27 | 10.9 | 93.80 | 5.73 | 3 |
| | | 340 | 10 | 90 | 150 | 100 | 5 | 7.8 | 94.57 | 6.00 | 5 |
| | | 340 | 10 | 90 | 150 | 100 | 22 | 0.0 | 92.93 | 6.87 | 5 |
| | | 340 | 10 | 90 | 150 | 100 | 5 | 12.1 | 93.70 | 7.13 | 7 |
| | | 340 | 10 | 90 | 150 | 100 | 22 | 16.5 | 92.47 | 8.17 | 7 |
| | | 340 | 10 | 90 | 100 | 110 | 10 | 16.6 | 93.23 | 8.43 | 8 |
| 340 | 3 | 90 | 150 | 110 | 10 | 7.7 | 92.08 | 10.45 | 10 | | |
| 10 | 17 | 90 | 100 | 110 | 5 | 1.4 | 92.00 | 12.35 | 12 | | |

Table 1. Summary of the seismic scenarios used to simulate the 2004 Indian Ocean tsunami. Fault mechanisms for Scenario A from Grilli et al. (2007) and Scenario B from Tanioka et al. (2006).

125 ios 1 and 2 which account for the energy accumulated along the fault plane since 1833, taking into account the energy
 released due to the 2007 Bengkulu earthquake.

2. Arakan Subduction Zone

130 Two plausible fault mechanisms capable of tsunamigenesis with implications in the far-field are simulated for the the
 Arakan subduction zone (Table 2). Scenario 3 represents the fault mechanism for the 1762 Bangladesh-Myanmar earth-
 quakes. Scenario 4 represents a less probable, but plausible fault mechanism accounting for the residual energy from the
 2004 megathrust event. Despite the lack of evidence that a large tsunami greater than 2 m in the Maldives could originate
 from the Arakan Subduction zone due to the bathymetry of the Bay of Bengal (Okal and Synolakis, 2008), we include
 these scenarios that originate in the Arakan Subduction Zone as RMSI (2006) predicts tsunamis from this region to have
 the shortest return period with significant impact to the Maldives amongst all the regions of origin considered in this
 135 study.



| Scenario | M_0 | Φ | δ | λ | L | W | h | ΔU | Source Center | |
|--|-----------------------|--------|----------|-----------|------|------|------|------------|----------------|-----------------|
| | (dyn X cm) | (deg) | (deg) | (deg) | (km) | (km) | (km) | (m) | Latitude (deg) | Longitude (deg) |
| Seismic Zone : Southern Sumatra | | | | | | | | | | |
| 1 | 6.3×10^{29} | 322 | 12 | 90 | 550 | 175 | 15 | 13 | 100.85 | -2.05 |
| 1a | 1.7×10^{29} | 322 | 12 | 90 | 350 | 175 | 15 | 6 | 100.85 | -2.05 |
| 2 | 1.13×10^{30} | 322 | 12 | 90 | 900 | 175 | 15 | 15 | 101.00 | -2.80 |
| 2a | 6.0×10^{29} | 322 | 12 | 90 | 900 | 175 | 15 | 8 | 101.00 | -2.80 |
| Seismic Zone : Arakan | | | | | | | | | | |
| 3 | 1.5×10^{29} | 324 | 20 | 124 | 470 | 100 | 10 | 6.5 | 93.45 | 19.80 |
| 4 | 2.8×10^{29} | 20 | 15 | 90 | 470 | 175 | 10 | 7 | 95.29 | 15.39 |
| Seismic Zone : Makran | | | | | | | | | | |
| 5 | 1.9×10^{29} | 265 | 7 | 90 | 550 | 100 | 15 | 7 | 64.00 | 25.30 |
| 6 | 3.9×10^{29} | 265 | 7 | 90 | 550 | 100 | 15 | 7 | 64.00 | 25.30 |
| | | 280 | 7 | 90 | 450 | 150 | 30 | 6 | 59.43 | 25.98 |

Table 2. Summary of the eight plausible fault mechanisms across the Indian Ocean proposed by Okal and Synolakis (2008), which we consider in this study.

3. Makran Subduction Zone

We consider two fault scenarios originating from the Makran subduction zone. Scenario 5 considers the combined mechanisms of the ruptures in the three most eastern zones of the fault line as per Byrne et al. (1992), which corresponds to the combined fracture zones triggering the the 1851–1864, 1945 and 1765 earthquakes. Scenario 6 further adds the plausible fault zone corresponding to the 1483 earthquake, extending the fault line further west. RMSI (2006) predicts relatively long return periods for tsunamis that impact upon the Maldives that originate from the Makran subduction zone, with a return period just over 250 years for a tsunami with amplitudes of 2 m in the Maldives.

2.3 Numerical Simulations

In this study we use Thetis, a 2D (Angeloudis et al., 2018) and 3D (Kärnä et al., 2018; Pan et al., 2019) flow solver, built using the Firedrake finite element solver platform (Rathgeber et al., 2016) to carry out numerical simulations. Here we use the 2D version of Thetis and solve the depth-averaged shallow water equations in non-conservative form :

$$\frac{\partial \eta}{\partial t} + \nabla \cdot (H_d \mathbf{u}) = 0, \quad (1)$$

$$\frac{\partial \mathbf{u}}{\partial t} + \mathbf{u} \cdot \nabla \mathbf{u} - \nu \nabla^2 \mathbf{u} + f \mathbf{u}^\perp + g \nabla \eta = -\frac{\tau_b}{\rho H_d}, \quad (2)$$



where η is the free surface displacement (m), H_d is the total water depth (m), \mathbf{u} is the depth-averaged velocity (ms^{-1}),
150 comprising the x - and y -components u and v , and ν is the kinematic viscosity of the fluid ms^{-1} . The term $f\mathbf{u}^\perp$ accounts for
the Coriolis force, where $f = 2\Omega\sin(\zeta)$, with Ω the angular rotation of the Earth, ζ the latitude and \mathbf{u}^\perp the velocity vector
rotated 90° .

The model uses a discontinuous Galerkin finite element discretization (DG-FEM), using the $\text{P}_1^{\text{DG}}\text{-P}_1^{\text{DG}}$ velocity-pressure
finite element pair. For time-stepping, a semi-implicit Crank-Nicolson approach is applied with a constant time step of Δt . For
155 all simulations a time step of $\Delta t = 5$ s was used.

The model treats wetting and drying according to the formulation of Kärnä et al. (2011), which introduces a modified
bathymetry $\tilde{h} = h + f(H)$, ensuring a positive total water depth in the model equations, with $f(H)$ defined as:

$$f(H) = \frac{1}{2}(\sqrt{H^2 + \alpha^2} - H), \quad (3)$$

where H is the water height, and α is a tunable constant which for all simulations in this work was set to $\alpha = 2.0$.

160 Bed shear stress τ_b is implemented through the Manning's n formulation as

$$\frac{\tau_b}{\rho} = gn^2 \frac{|\mathbf{u}|\mathbf{u}}{H_d^{1/3}}. \quad (4)$$

To derive the free surface elevation from the fault parameters, we use the Okada analytical formulae (Okada, 1992) and
assume that the initial instantaneous free surface water displacement is equal to the sea floor displacement and impose these as
either the initial condition or at the appropriate time in the model (table 1).

165 2.3.1 Model Setup

Each scenario was run in a full simulation which spatially extended across the Indian Ocean as seen in Figures 2 (a) and 1 (a),
as well as a nested simulation focused on the Maldives archipelago, as seen in Figures 2 (b) and 1 (b). Absorbing boundary
conditions were set using a sponge region of increased viscosity at the open boundaries of the full simulation. For the nested
simulation, tsunami amplitudes from the full simulation were used to force the model at the domain boundary depending on the
170 direction of the tsunami wave, i.e. here a one-way coupling approach was employed. Tidal forcing was not taken into account,
as earlier studies of tidal amplitudes (Rasheed et al., 2020), have shown that the tidal regime of the region is very small, with
maximum variations of 1 m from the mean sea level.

2.3.2 Bathymetry

We used the GEBCO 2019 global bathymetry data set (Weatherall et al., 2015), as seen in Figure 1 (a), for the large-scale
175 simulation but a finer bathymetry dataset is essential to run meaningful regional hydrodynamic simulations at the scale of
Atolls and islands. This is particularly important for the complex Atoll systems of the Maldives archipelago where bathymetry
can vary from being at sea level to extreme depths within a small spatial distance. The high resolution bathymetry dataset of
the Maldives of Rasheed et al. (2020) and shown in Figure 1 (b) is therefore used for the nested simulations. The use of this
new bathymetry dataset is essential: field studies by Riyaz et al. (2010) and Riyaz and Suppasri (2016), which analysed various

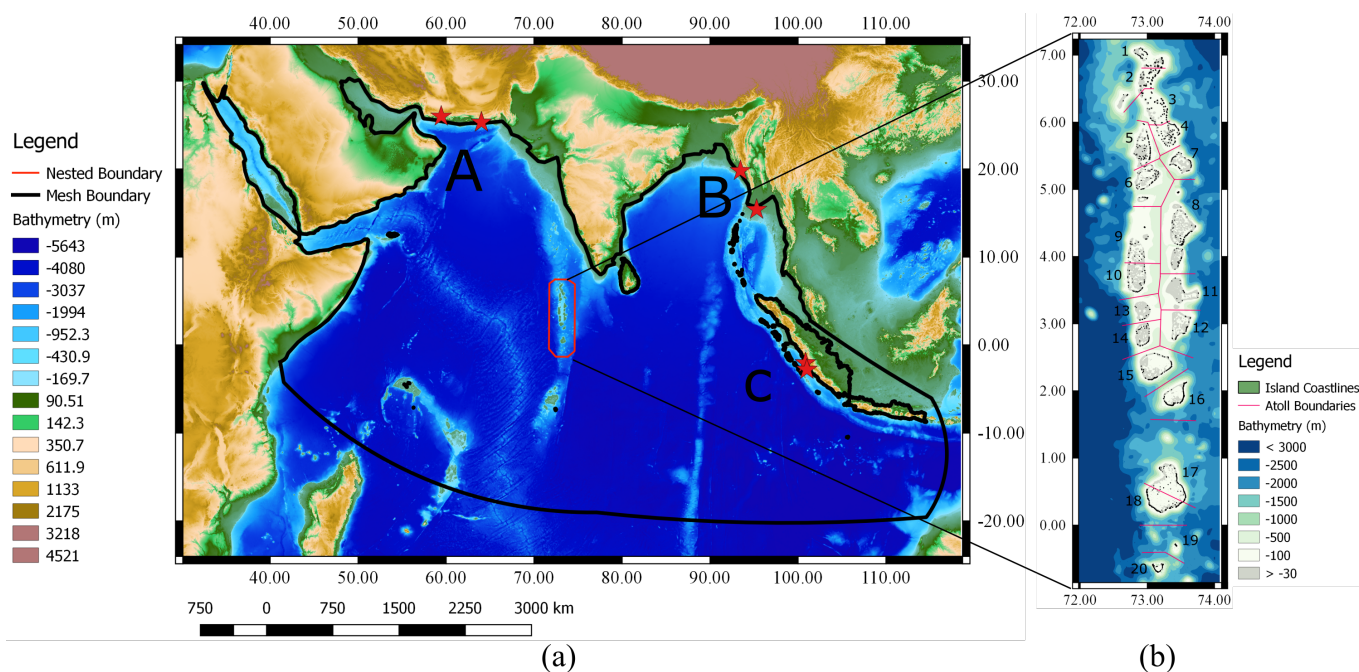


Figure 1. (a) Bathymetry of the Indian Ocean and topography of the region from GEBCO 2019 (Weatherall et al., 2015) and (b) the bathymetry of the Maldives as per Rasheed et al. (2020) used for the nested high resolution modelling. The seismic zones of fault origins (marked by red stars) are labelled in (a) as A: Makran Subduction Zone, B: Arakan Subduction Zone and B: South Sumatra Subduction Zone. The current administrative Atoll boundaries of of the Maldives archipelago is shown in (b) and labelled using official names as 1. North Thiladhunmathi, 2. South Thiladhunmathi, 3. North Miladhunmadulu, 4. South Miladhunmadulu, 5. North Maalhosmadulu, 6. South Maalhosmadulu, 7. Faadhippolhu, 8. Male', 9. North Ari, 10. South Ari, 11. Felidhe', 12. Mulaku, 13. orth Nilandhe, 14. South Nilandhe, 15. Kolhumadulu, 16. Hadhunmathi, 17. North Huvadhoo, 18. South Huvadhoo, 19. Fuvahmulah and 20. ddu Atoll.

180 statistical correlations between island size, shape, distance to reef edge with respect to the impact of the 2004 Boxing Day
 tsunami across the Maldives, suggested that small scale features present within the Atolls likely affect wave propagation and
 therefore tsunami impact. Fujima et al. (2006) carried out a numerical simulation of the 2004 tsunami event using a bathymetry
 dataset with a spatial resolution of 2 arcminutes and highlighted the need for more accurate bathymetry data to account for the
 complex bathymetry of the Atolls. The bathymetry dataset used here has been used previously for hydrodynamic modelling
 185 of the Maldives at the Atoll (Rasheed et al., 2020) and archipelago-scale (Rasheed et al., 2021), and has been successfully
 validated against qualitative and quantitative field data.

2.3.3 Coastline data

The simulation domain contains a wide variety of coastlines, ranging from numerous small islets in the range of 10 s of metres
 to continental shorelines in the range of 1000 s of kilometres. Following the study by Rasheed et al. (2021), we used the GADM
 190 database (Areas, 2018), as illustrated in Figure 1 (b), to represent the coastlines of the islands of the Maldives in the nested

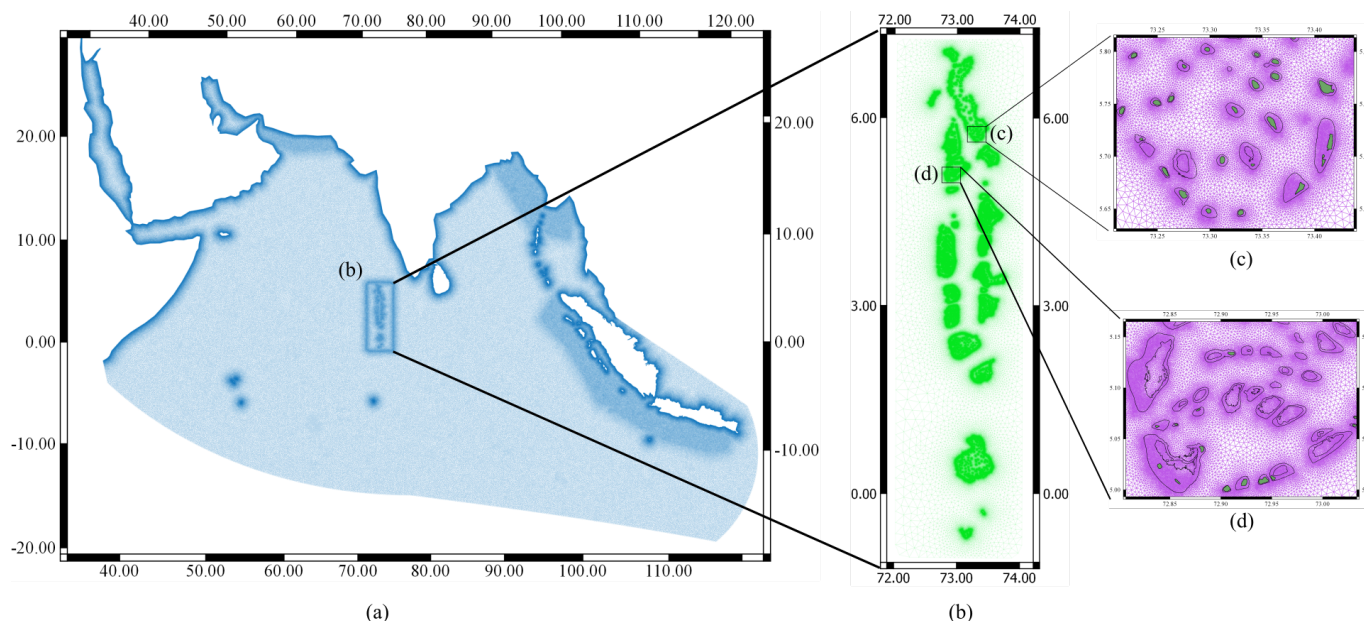


Figure 2. (a) The unstructured mesh used for the full simulation, showing increased mesh resolution around fault zones, and coastal areas. (b) The unstructured mesh used for the nested simulations showing increased resolution near the Maldives archipelago. Panel (c) highlights discontinuous reefs of South Midhunmadulu Atoll while panel (d) zooms in on the unique faro system of South Maalhosmadulu Atoll.

simulation and no islands or islets were removed. For the full simulation, we used the "low" resolution GSHHG coastline data from Wessel and Smith (2013), Figure 1 (a), from which we removed smaller islands as the emphasis of this study is the impact of potential tsunamis across the islands of the Maldives archipelago and large-scale propagation is not affected by the presence of small scale islands.

195 2.3.4 Bed friction

A uniform Manning friction parameter of $0.025 \text{ s m}^{-1/3}$ was applied across the domain for both the full and the nested simulations, and the minimum water depth was set as 0.1 m, applying a quadratic drag coefficient (C_D) that varies with the bathymetry, between ~ 0.0005 in the open ocean to ~ 0.026 in shallow areas. These values are in line with Kraines et al. (1998), who reported similar values in shallow water lagoons and reefs characteristic of the Maldives. Dilmen et al. (2018),
200 studied the impact of bed friction on tsunami amplitudes in a reef environment and found that the use of different bed friction values yield varying results within different geographic areas in a reef environment. Here, we use these generic values, as bed friction for coral Atolls such as that of the Maldives are not sufficiently known (Rosman and Hench, 2011).



2.3.5 Unstructured mesh generation

The Python package *qmesh* (Avdis et al., 2016, 2018) was used to generate the meshes used for the simulations within this work. The mesh for the full simulation, shown in Figure 2 (a), contains 444,865 nodes and 889,852 triangular elements. The meshes were generated in the UTM43N coordinate reference system and the mesh element size was set to 15 km in the open regions and a refinement of 2500 m was applied towards continental coastlines and large islands. A further refinement of 5000 m and 7500 m was set at the Atoll boundaries of the Maldives archipelago and fault regions. Very small features such as small islands were excluded from the full simulation mesh, while all islands of the Maldives were included in the nested simulation (see section 2.3.3).

For the higher resolution nested simulation covering the Maldives area, we use a high resolution mesh which contains 1,156,656 nodes and 2,314,856 triangular elements. The mesh element size varied from 10 km at the open boundaries to 50 m at the coastline of the islands of the Maldives. Further refinement of 100 m was applied towards the shallow lagoon areas as shown in Figure 2 (b1) and (b2). These mesh refinement scales were selected based on the mesh resolution study by Rasheed et al. (2021), which showed that this scale of refinement is necessary to fully capture the numerous small scale features of the complex Atolls of the Maldives.

3 Results

3.1 Simulations of the 2004 Boxing Day tsunami

The Indian ocean tsunami of 2004 provides observational data, which can be used for model validation purposes. Various investigators have gathered field data across the Maldives archipelago documenting the aftermath of the 2004 tsunami. Since we here use both qualitative and quantitative data from these sources, we first present a brief summary of surveys carried out in the Maldives that report tsunami amplitudes at different points across the archipelago and then compare results from the 2004 Boxing Day simulations with these field observations.

3.1.1 Observed tsunami amplitudes from field surveys

Fritz et al. (2006) carried out a field survey across 11 islands in the central Maldives, which included the islands worst affected by the 2004 Boxing Day tsunami. The survey noted that the low-lying nature of the islands, likely combined with the local bathymetry, resulted in complete flooding of the islands surveyed and that classic tsunami features such as different inundation lines at different elevations and tsunami run-up could not be observed. The maximum tsunami heights reported in the study are of order 1 to 4 m but these were noted to be less than half of the values reported in east Africa at almost twice the distance.

Fujima et al. (2006) carried out a similar survey across seven Maldivian Atolls, with similar conclusions to Fritz et al. (2006). The survey of Fujima et al. (2006) also included locations with tide gauges in the North, South and Central regions of the archipelago. The survey results of Fujima et al. (2006) highlight the high degree of regional variability of the tsunami amplitudes along the coastlines and between islands, even if the islands show little variation in topography. For instance, the

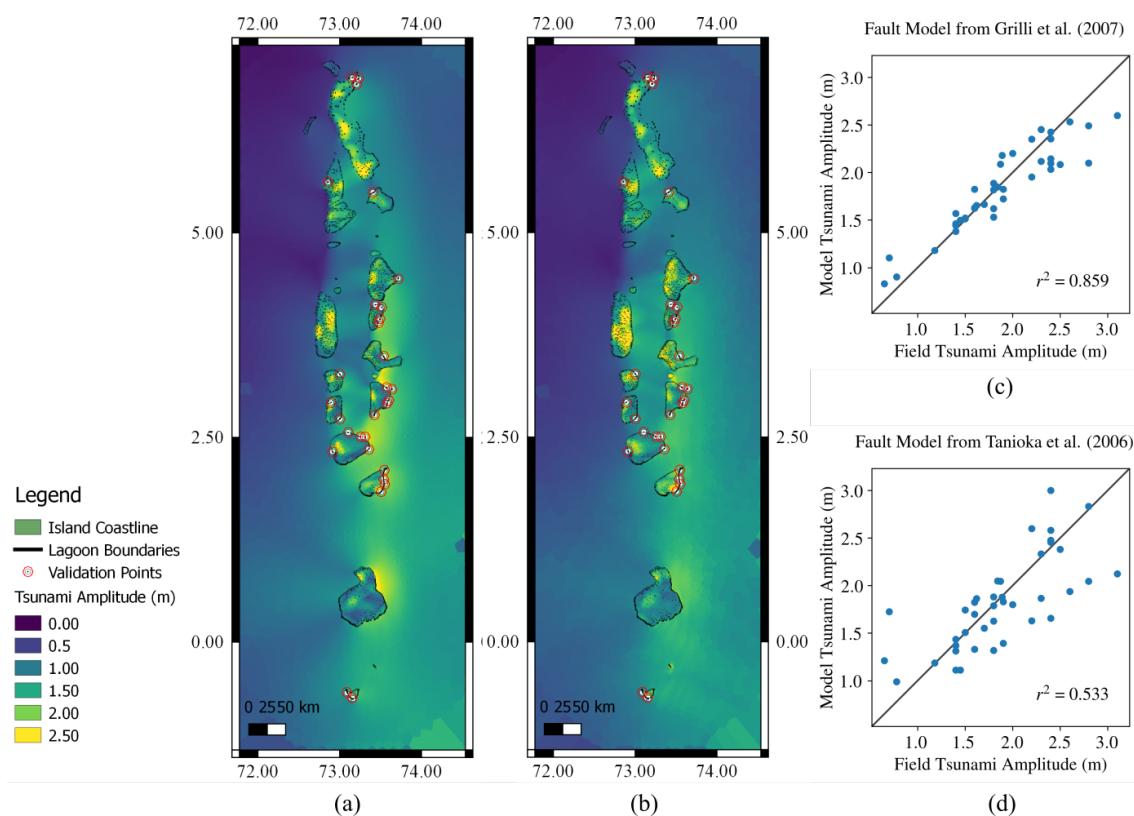


Figure 3. Maximum tsunami amplitude across the Maldives, modelled using (a) the fault model described in Grilli et al. (2007) (scenario A) and (b) a multi-scale fault model described in Tanioka et al. (2006) (scenario B). Panels (c) and (d) compare simulated tsunami amplitudes with observations from field surveys for 41 validation points, for scenarios A and B, respectively.

235 tide gauge in Gan Island, Seenu Atoll, recorded tsunami amplitudes of less than 1 m but survey results from the field study revealed that tsunami amplitudes across the island in the vicinity of the tide gauge varied by more than 1 m.

Kan et al. (2007) carried out an extensive survey across 43 islands of the archipelago to observe the impact of the tsunami, focusing on islands along the eastern rim of the archipelago, where the initial tsunami surge hit the islands. In addition to inundation heights, the Kan et al. (2007) survey also reports the cross-sectional topography of the islands for the locations surveyed, providing a snapshot of the tsunami wave in the local vicinity of the islands and the impact of local topography on
240 inundation across the islands.

Survey results from all of these field studies are included here, however, where the spatial distance is very small, we considered the measurement which was closest to the coastal line, since the model used here is capable to propagate up to the coastline (explicit simulations of inland flooding would require an even higher resolution representation of land feature and additional dynamics).



245 3.1.2 Comparison of the model simulations with field observations

Comparison of model results with field data indicates that the results using the fault model of Grilli et al. (2007) and the more complex fault model of Tanioka et al. (2006) are consistent in predicting the regions of maximum impact across the archipelago (Figure 3 (a) and (b)). Both simulations predict large variations in tsunami amplitude across very small spatial distances, in line with field observations, and consistent with expectations given the complex nature of the bathymetry and coastline of the islands, which is for the first time incorporated in these high-resolution results.

To quantitatively compare the performance of the two models, the Pearson correlation coefficient defined as:

$$r = \frac{\sum_{n=1}^N (O_n - \bar{O})(M_n - \bar{M})}{\sqrt{\sum_{n=1}^N (O_n - \bar{O})^2 \sum_{n=1}^N (M_n - \bar{M})^2}}, \quad (5)$$

where N is the number of data points, O_n and M_n are the observed and modelled values and \bar{O} and \bar{M} are the means of the observed and modelled values was used to quantify agreement in tsunami heights between the two simulations for the 2004 event at 41 locations across the country, where field data is available. Comparison results, in figure 3 (c) and (d), shows that a Pearson correlation coefficient of 0.9 was obtained for the square of the correlation coefficient (r^2) for scenario A (using the fault model by Grilli et al. (2007)) while the corresponding value obtained for scenario B (using the fault model by Tanioka et al. (2006)) is 0.73, showing that the maximum tsunami elevations are highly sensitive to fault parameters.

We also note that the islands of south eastern Kolhumadulu Atoll, north eastern Mulaku Atoll and the eastern Hadhunmathi Atoll are shown by the model to experience the maximum impact (Figure 3). Kan et al. (2007) reports that the islands in this zone experienced the maximum damage across the archipelago, observations that are consistent with the model outputs obtained here. Out of the 106 persons either missing or known to have died across the archipelago, this region alone accounted for at least 78. The islands on the north eastern zone of Huvadhu Atoll (Figure 4 (a) and (e)) were both inhabited and also reported fatalities; the model simulations also predict high tsunami amplitudes there. The south eastern zone of South Nilande Atoll as well as the inner Atoll basin regions of several Atolls, such as North Maalhos Madulu and South Nilande Atoll, are also predicted by the model to have high maximum tsunami amplitudes.

3.1.3 Difference in local tsunami amplitude due to two different faulting mechanisms

With a distance of over 2000 km from the fault origin, the Maldives qualifies as far-field for the 2004 Indian ocean tsunami and the use of different fault models is generally not expected to result in significant differences (Okal and Synolakis, 2008). However, we observe differences in maximum tsunami amplitudes for the simulations when the fault model is changed as seen in (Figure 3 and Figure 4). These differences arise from differences in the seismic moment and fault geometry inherent to the two fault models (see Table 1).

This is in line with results from Poisson et al. (2011), who also found differences in modelled tsunami amplitudes across the coast of Sri Lanka when different fault mechanisms were used for the 2004 event. Figure 4 (a–h) shows maximum tsunami amplitudes simulated across various locations for both fault models, indicating that the more energetic fault model by Grilli et al. (2007) leads to a general increase of maximum tsunami amplitude across the domain. However, the maximum tsunami

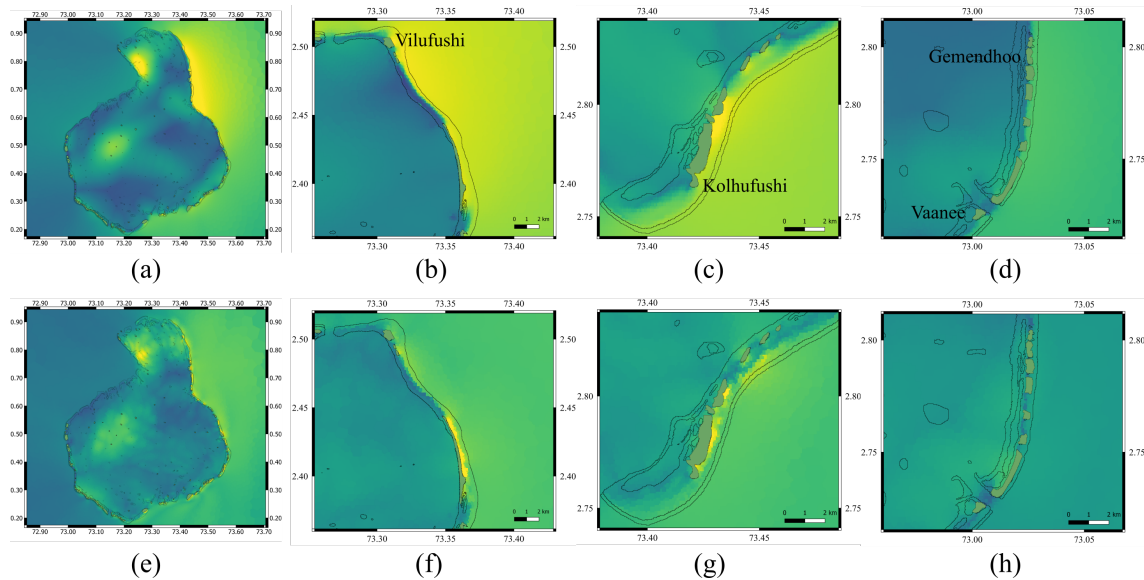


Figure 4. Maximum Tsunami amplitude across (a) Huvadho Atoll, and the region around the islands of (b) Villufushi (North East Kolhumadulu), (c) Kolhufushi (south eastern Mulaku Atoll), (d) Vaanee and Gemendhoo (south eastern zone of South Nilande Atoll), using the fault model by Grilli et al. (2007) and (e–h) using fault model by Tanioka et al. (2006).

amplitudes simulated with the fault model by Tanioka et al. (2006) predicts higher amplitudes in some areas. Figure 4 (b) and (c), showing the maximum tsunami amplitude in the vicinity of the hard-hit Kolhufushi island (south eastern zone of Mulaku Atoll), illustrate this phenomenon.

280 The fault models differ in their direction of focus. Figure 4 (b) shows significant increase in amplitude in the north eastern part of Kolhumadulu Atoll, an area which suffered devastation during the event, destroying the inhabited island of Villufushi and significantly altering the geomorphology of the uninhabited island of Kalhufahalaafushi to the South. However, figure 4 (f), shows that the fault model of Tanioka et al. (2006) focuses the maximum impact across the island of Kalhufahalaafushi, leading to no significant increase in tsunami amplitude simulated for Villufushi island.

285 3.2 Impact of various tsunami scenarios from around the Indian Ocean on the Maldivian archipelago

1. Southern Sumatra Subduction Zone

We find that the impact across the Maldives archipelago for the worst case tsunami scenarios simulated with origin in the South Sumatra subduction zone is significantly less in comparison to the 2004 event. However, worst case scenarios of South Sumatra origin can produce tsunamis which can have an impact in the Maldives. The lower severity of waves produced by earthquakes along the Southern Sumatra subduction zone is due to the tsunami wave direction which, in this case, is focused away from the Maldives and towards the south western Indian Ocean (Okal and Synolakis, 2008).

290

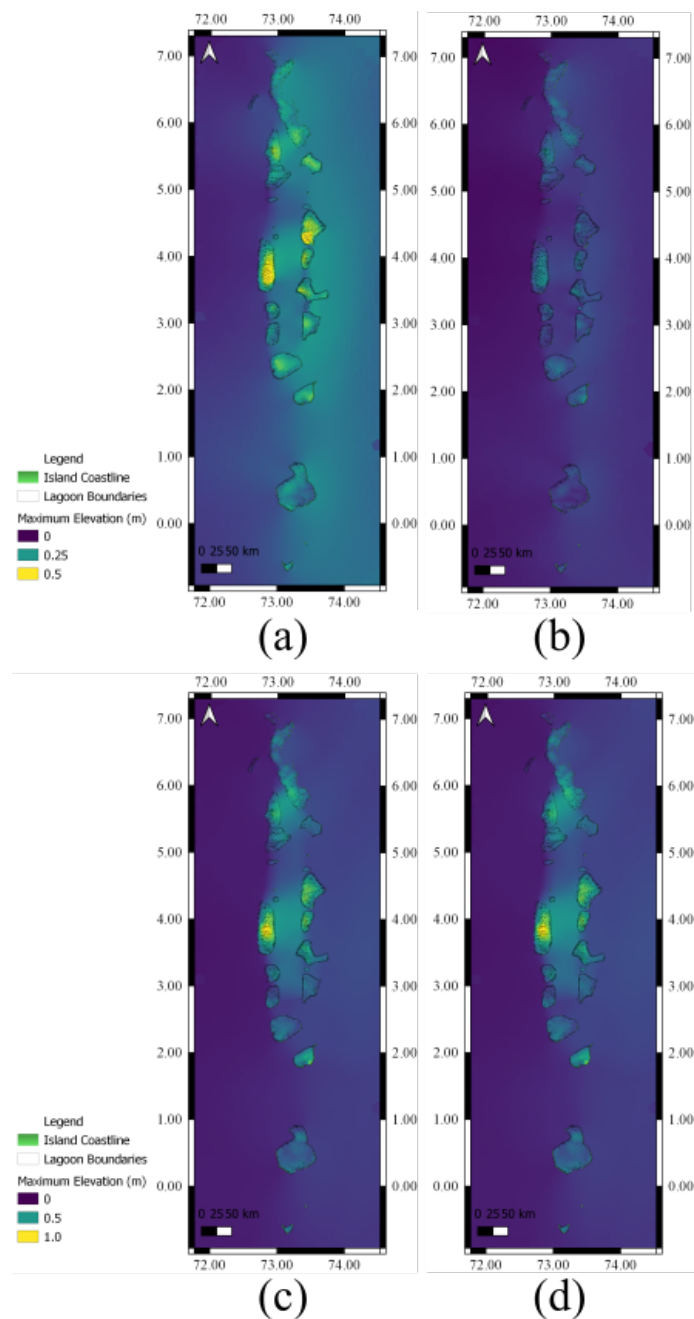


Figure 5. Maximum tsunami amplitude across the Maldives for (a) scenario 1, (b) scenario 1b, (c) scenario 2 and (d) scenario 2b from Table 2. Even for the worst case scenarios the maximum tsunami amplitude is relatively small.

Scenario 1 (Figure 5 (a)) is a tsunami simulation of the 1833 South Sumatra earthquake. This event is predicted to have little impact for the Maldives, with maximum local tsunami amplitudes averaging only 0.5 m (Figure 5 (a)). South Male



295 Atoll, central regions of North Maalhosmadulu Atoll and Ari Atoll are predicted to suffer the greatest impact, but even then the predicted amplitude is relatively small and there exist no records of damage in the Maldives for that 1833 event. Scenario 1(a), which simulates the more recent Bengukulu earthquake (2007) also produces very small amplitudes across the Maldives (Figure 5 (b)) and warrants no further discussion.

300 Scenario 2, which represents a plausible extension of scenario 1, leads to larger impacts across the archipelago (Figure 5 (c)), particularly for Atolls located in the central region, with tsunami amplitudes close to or exceeding 1 m at some locations, due to the tsunami being directed towards this region. Given that the maximum tsunami amplitude distribution simulated for that event is similar to the 2004 Indian ocean tsunami, one would expect that tsunamis generated by an event similar to scenario 2 could lead to significant damage. Scenario 2a, which is a modification of scenario 2 that reduces the total energy of the tsunami, accounting for the 2007 Bengkulu earthquake, leads to reduced tsunami amplitude predictions across the Maldives as expected, but the forecasted amplitudes in the Maldives region are still
305 higher than those predicted for scenario 1. If combined with a high tide, tsunamis generated by scenario 2a would likely have an impact across locations predicted to have higher amplitudes.

2. Arakan Subduction Zone

Two fault scenarios were considered in the Arakan subduction zone as described in Table 2. Scenario 3 considers the fault mechanism involved in the 1762 earthquake, and scenario 4 simulates a plausible fault to the North of the 2004
310 boxing day event. As predicted by Okal and Synolakis (2008), simulated amplitudes for both scenarios are relatively small across the Maldives (Figure 6). This result is in line with simulations predicting that tsunamis originating from the Arakan subduction zone do not propagate away from the Bay of Bengal due to the seafloor bathymetry (Okal and Synolakis, 2008). Given that the maximum tsunami amplitudes of the worst case scenarios in the Arakan subduction zone are minimal, this suggests that earthquakes from the Arakan subduction zones are not likely to be a significant
315 threat to the Maldives.

3. Makran Subduction Zone

Scenario 5 simulates the 1945 Makran tsunami originating from an earthquake along the Makran subduction zone. Simulation results from this scenario indicate that tsunamis with this origin can have a substantial impact in the Maldives (Figure 7 (a)), particularly across the Northern Atolls of the Maldives. We also find that due to the bathymetry of the
320 Arabian sea, tsunami waves originating there reach the Northern Atolls of the Maldives before reaching regions that are closer in proximity, such as major cities along the coast of western India. Localised maximum tsunami amplitudes are predicted to be close to 1 m for some key islands of the Northern Maldives. We conclude that earthquakes from the Makran subduction zone could cause considerable damage, especially if combined with high tidal conditions.

325 It is plausible that the damage due to the 1945 event in the Maldives was left undocumented due to the fact that the most impacted region was mostly uninhabited at the time. However, it is expected that events of this amplitude would have a considerable impact on infrastructure if repeated today. For example, Hanimaadhoo Island, which today hosts

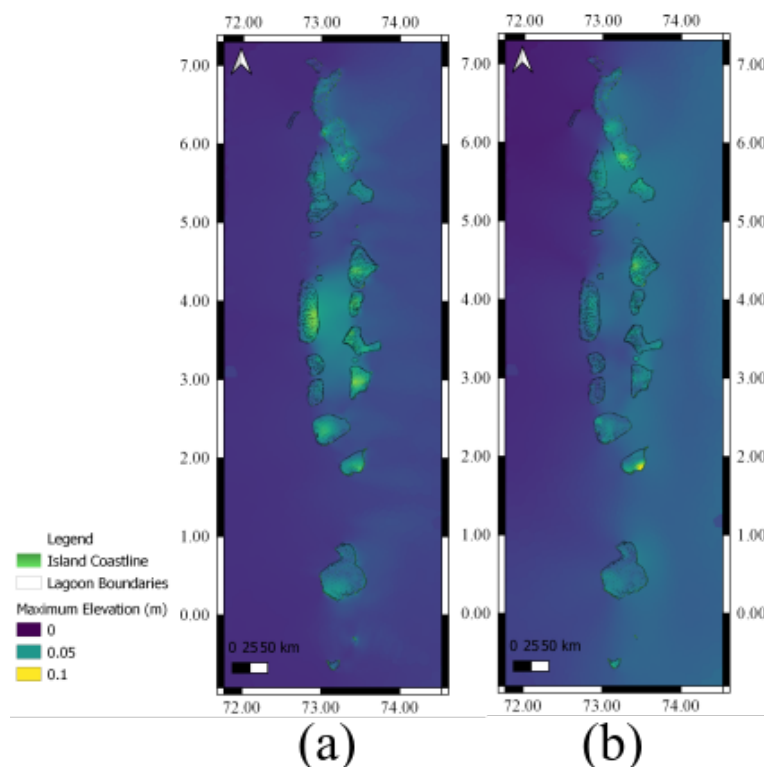


Figure 6. Maximum tsunami amplitude across the Maldives due to plausible worst case fault case scenarios in the Arakan Subduction zone, corresponding to scenarios 3 and 4 from Table 2.

the only International Airport in the Northern Maldives, would be expected to face tsunami waves of 0.8 m. Further, the islands of the Northern Atolls of the Maldives are more populous in comparison to the Southern regions of the Maldives. Our results for scenario 5, coupled with recent increases in the populations of some of the impacted areas, indicate that Makran area earthquakes represent a new risk for the Maldives.

330

Maximum tsunami amplitudes simulated for scenario 6, which represents an extended fault system in addition to the 1945 earthquake, is predicted to have a slightly smaller impact than scenario 5, in agreement with results by Okal and Synolakis (2008) (Figure 7 (b)). The smaller impact of this larger earthquake generating mechanism is due to destructive interference of the waves near the source.

335

Even though tsunamis with origin in the Java Subduction zone are predicted to produce waves with implications in the far-field (Okal and Synolakis, 2008), the impact of these tsunamis across the Maldives is predicted to be negligible, in line with similar studies in the region such as Wijetunge (2012) in Sri Lanka.

Further, even though a number of transformation faults exist along the South western Indian Ocean Ridge (SWIO), and some of the world's largest earthquakes have been recorded at these locations, according to Okal and Synolakis (2008),

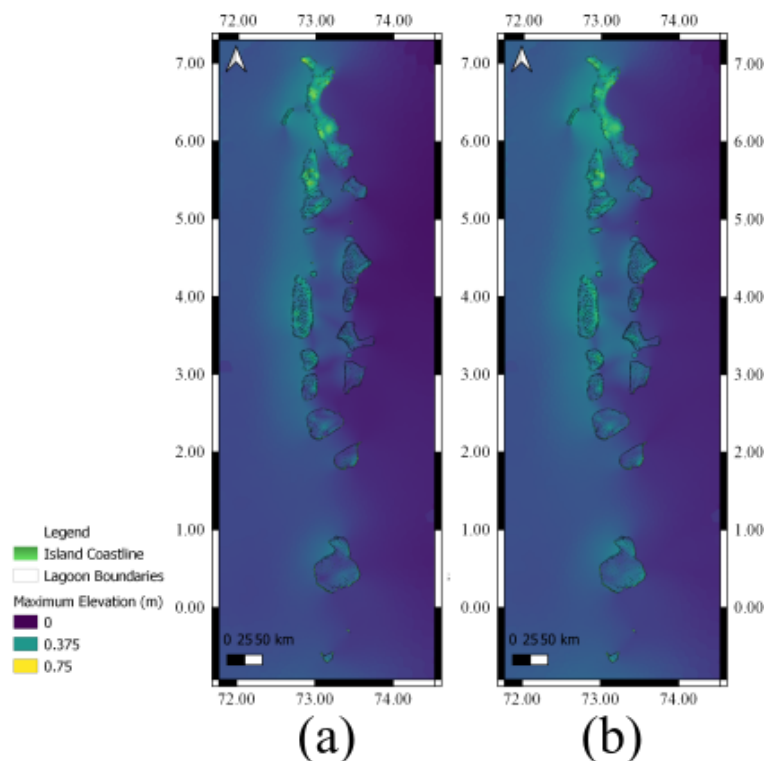


Figure 7. Maximum Tsunami amplitude across the Maldives at due to plausible worst case fault case scenarios in the Makran Subduction zone, corresponding to (a) scenario 5 and (b) scenario 6 from Table 2.

340 none of these are capable of generating tsunamis that impact upon the far-field. Here we exclude Calrseberg Ridge as
a plausible fault mechanism on account that RMSI (2006) predicts return periods of ≈ 400 years for a tsunami with
amplitude greater than 1.5 m in the Maldives area.

4 Discussion

4.1 Importance of local and regional bathymetry-induced refraction/diffraction patterns in modulating the local 345 impact of the 2004 Boxing Day event

The use of a high resolution bathymetry dataset of the archipelago allows the simulation of tsunami characteristics hitherto
not modelled at this scale. Here we summarise and compare some of the observations from the model which demonstrates
refraction, diffraction and reflection patterns within the Atolls and show how these contribute to zones of maximum impacts
during the 2004 Boxing Day event.

350 The simulation using the fault model defined by Grilli et al. (2007) are used here to discuss the impact of the 2004 tsunami
event in more detail since these yielded better correlation results when comparing data to model results.

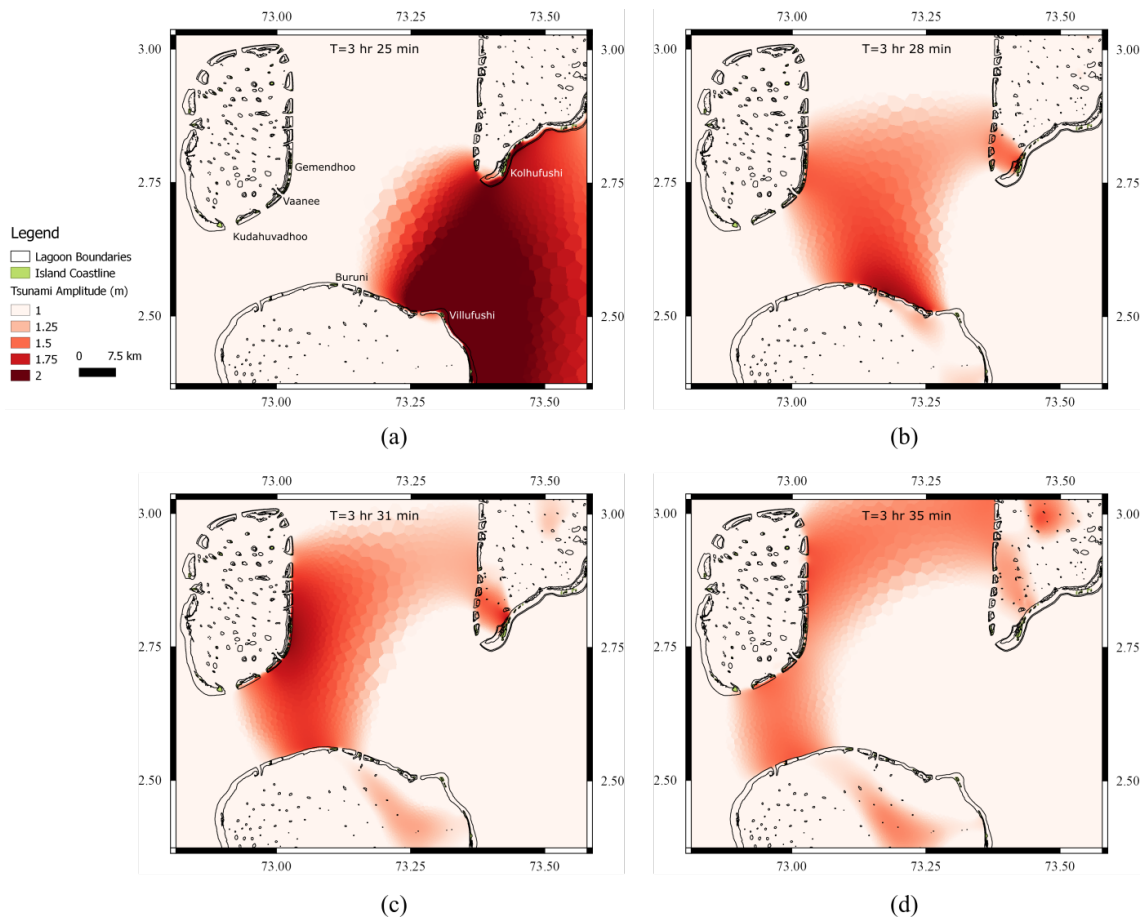


Figure 8. The 2004 boxing day Tsunami propagation across *Kudahuvadho* *Kandu* (Sea of *Kudahuvadho*) (the junction of South Nilande Atoll, Mulaku Atoll and Kolhumadulu Atoll) at (a) $T=3\text{hr } 25\text{min}$, (b) $T=3\text{hr } 28\text{min}$, (c) $T=3\text{hr } 31\text{min}$, (d) $T=3\text{hr } 35\text{min}$. (a) shows the high tsunami amplitude across Kolhufushi island in Mulaku Atoll and Villufushi island in Kolhumadulu Atoll. (b–d) shows the formation of a bow wave across the channel between Mulaku and Kolhumadulu Atolls, which propagates towards Vaanee and Gemendhoo island in south eastern part of South Nilande Atoll.

The steep bathymetry of the Maldivian Atolls and the geomorphology of the lagoons is extremely efficient at reducing the impact of tsunamis at the island scale. This is demonstrated by the fact that, of the various individual scenarios are simulated in this study, none is predicted to have as high an impact across the Maldives as the mega 2004 event, highlighting that the geographic features of the Maldives archipelago naturally attenuate the impact of far-field tsunamis, and extremely large events are required to breach the natural defenses offered by the natural geomorphology of the lagoon, in spite of the low elevation of the islands themselves.

However, the simulations conducted also clearly demonstrate that the location and shape of Atolls plays an important role in amplifying and focusing the tsunami impact locally. The location of Kolhufushi Island in South Mulaku Atoll, combined with



360 the shape of Kolhufushi lagoon, causes water to build up across the island as seen in Figure 4 (c), (g) and Figure 8 (a). A similar observation is made in Villufushi Island in North Eastern Kolhumadulu Atoll across the channel. The location of the island, in a headland (*Villufusi Muli*) (Luthfee, 1995) projecting out to the area of primary tsunami impact, causes tsunami amplitudes to build up between these islands. These two islands (Kolhufushi and Villufushi), where maximum tsunami amplitudes were recorded across the archipelago, were the only two islands to record double digit figures for people dead or missing.

365 We also observe that the geometry of north eastern Kolhumadulu and south western Kolhumadulu Atoll forces a surge in tsunami amplitude along the south eastern rim of South Nilande Atoll, as seen in Figure 8 (a)–(d). Both inhabited islands in the region, Gemendhoo and Vaanee, were completely destroyed during the tsunami and remain uninhabited today.

Model predictions show that while the amplitude of the tsunami is lower at the south western zone of South Nilandhe Atoll in comparison to the eastern rim of Mulaku, Kolhumadulu and Hadhunmathi Atolls, the build-up of the tsunami surge persists
370 across this region for a longer period of time, due to the very shallow bathymetry of the region with depths less than 3 m. Further, the geomorphology of the region, which consists of a chain of small islets, is predicted to contribute to the build-up of the amplitude with high tsunami flow velocities across the shallow and narrow channels. On the other hand, we also find that Kudauhvadhoo Island in the south of South Nilande Atoll is predicted to have relatively low maximum tsunami amplitudes, in line with field surveys (Hmadhoon Hameed, 2005).

375 The shape of the Atoll and the location of the island within a large lagoon, as well as the steep bathymetry of the Atoll, caused the build-up of tsunami amplitude to pass through the channel between South Nilande Atoll and Kolhumadulu Atoll without any destructive impact to the island. Residents of both Gemendhoo and Vaanee were evacuated to Kudauhvadhoo on the day of the tsunami by the residents of Kudauhvadhoo and since then have been permanently relocated to the island. These simulations show that local and regional refraction and diffraction patterns can lead to vastly different outcomes, even for
380 neighboring islands of otherwise similar elevation.

Furthermore, we find that some of the field observations reported in the literature do not fully agree with other studies of tsunami hazard assessment across the Maldives based on statistical correlations between various parameters such as reef and island geomorphology. To illustrate, Kudauhvadhoo island discussed earlier is frequently predicted by (e.g., Riyaz et al., 2010; Riyaz and Suppasri, 2016) to be very vulnerable to tsunami impact, particularly for the 2004 Boxing Day event, while field
385 data and results of numerical modelling such as those conducted here, show that the island suffered no visible damage. Hence, we note that statistical correlations between various parameters such as the location of the island from the reef edge alone is not sufficient for tsunami vulnerability mapping for regions such as the Maldives, as these models do not account for the complex bathymetry of the reef environments which can sufficiently alter the local tsunami amplitude. Results of studies at other similar locations, also stress that tsunami wave characteristics are extremely complex. For example, Baba et al. (2008) found that
390 the Great Barrier Reef reduced the impact of the 2007 Solomon Islands tsunami by several orders of magnitude, while Ford et al. (2014) found that the level of attenuation offered by coral reefs depends on a variety of other factors, which statistical models do not take to account. In the present simulation domain of the Maldives archipelago, we find that the complexity of the tsunami wave propagation is amplified by the presence of numerous coral reefs within individual Atolls, as well as the presence of multiple Atolls within close vicinity.



395 The use of a high resolution bathymetry dataset allows the simulation to predict features such as an increase in tsunami
amplitudes due to shoaling as the tsunami passes through relatively shallow water contributing to increased damage. This is
evident in North Maalholmadulu Atoll, where a relatively shallow area with numerous coral reefs and faros is observed to
have larger amplitude tsunami waves than surrounding areas. The shoaling effect at Kandholhudhoo Island (the only inhabited
island in the zone), combined with a variety of other local factors, such as the absence of coastal vegetation and the removal
400 of reef for reclamation, lead to the complete destruction of the island; at the time this was the most densely populated island in
the Maldives. Similar predictions of higher tsunami amplitudes are made in the shallow water regions of western Ari Atoll and
western Kolhumadulu Atoll as seen in figure 3. However, as the islands at these locations were uninhabited at the time of the
Boxing Day tsunami, no field data exists for these regions against which to validate the model predictions.

We also observe that the model predicts diffraction and refraction wave patterns inside the Atoll basin, leading to high
405 amplitudes at islands which are not in the direct path of the tsunami. As seen in figure 3 (a), the central regions of South Nilande
Atoll is predicted to have a high tsunami amplitude. This is in agreement with eyewitness accounts and field observations at
Rinbudhoo island (Kan et al., 2007), where high inundation depths with the flow of water from all directions was reported.
Modelled results agree with these field observations and predict high tsunami amplitudes well within the central basin of the
Atoll. Simulation results predict that high tsunami amplitudes at this zone occurred due to the refraction patterns within the
410 the Atoll basin. Similar observations were made by Ford et al. (2014) based upon simulations of the 2011 Tohoku earthquake
in the Majuro Atoll in the Marshall Islands, where tsunami simulations exhibited long lasting tsunami amplitude peaks within
the Atoll for up to 60 minutes.

4.2 Atoll Tsunami Explorer Tool

Traditionally, the results of tsunami impact studies across the Maldives have been mainly represented via printed charts (e.g.,
415 RMSI, 2006; ADB, 2020; Riyaz et al., 2010; Riyaz and Suppasri, 2016). However, given the variation in tsunami impact across
the archipelago, interpretation of these charts to assess the nearshore impact across the coastline of islands, and especially to
assess island scale variations, is extremely difficult. To address this, we here present an interactive application tool built on the
Google Earth Engine (Gorelick et al., 2017) that can be used to explore the simulation results presented in this study.

The application, “Atoll Tsunami Explorer”, is hosted within the Island Health Explorer (I-Hex) platform (<https://i-hex.github.io>),
420 which brings together a host of similar interactive applications specific to the Maldives archipelago based on satellite imagery
and various other data sets. An illustration of the user interface of the “Atoll Tsunami Explorer” is shown in Figure 9. Users can
explore the maximum tsunami amplitudes at high resolution across the archipelago for any scenario described in this paper.
The tool was produced by uploading files generated from the simulation results to the Google Earth Engine platform. The
“Atoll Tsunami Explorer” is designed to be user-friendly and targets decision-makers as well as the wider community. To make
425 interpretation easier, the lagoon boundaries (Spalding et al., 2001) as well as the coastline files used in the simulation (Areas,
2018) are also added to the platform. Simulation results are clipped to the lagoon boundaries for better visualisation, however
an option is included that allows visualization of country-wide scenarios.

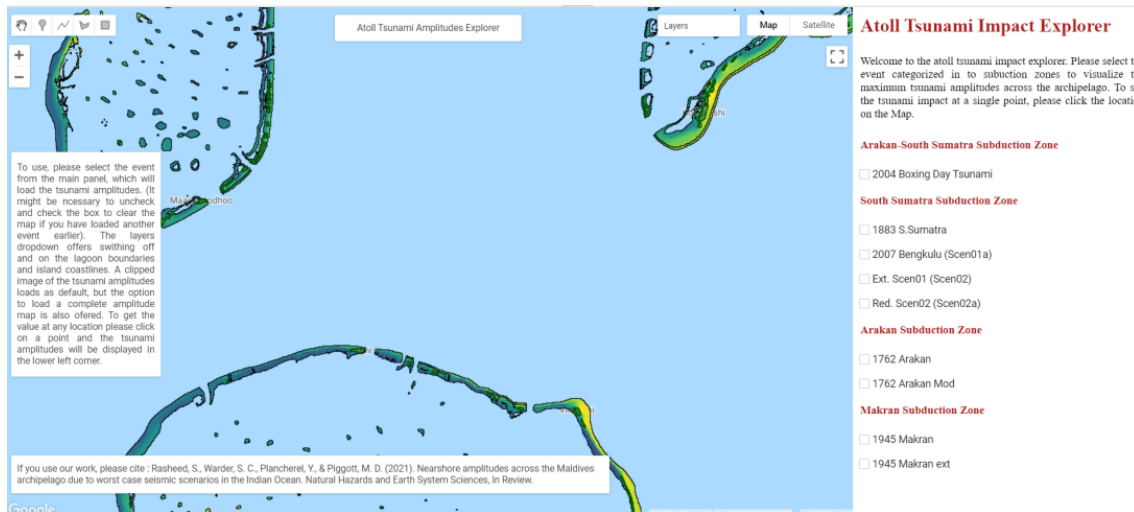


Figure 9. Atoll Tsunami Explorer based on the © Google Earth Engine platform, showing the default view with the 2004 tsunami amplitudes visualized with the lagoon and island boundaries.

4.3 Limitations of the Study and Recommendations for Improvement

The main limitation of this study is the lack of availability of suitable data both for model setup and validation, including bathymetry and bed friction fields. Even though the bathymetry dataset used (Rasheed et al., 2020) is the highest resolution currently available for the Maldives, it is comprised of data from a variety of sources and the defects of these datasets will manifest as defects in this study. We find that the bathymetry exerts a major influence in directing tsunami waves across the complex geometry of the Atolls of the Maldives, in agreement with Orpin et al. (2016), which showed similar effects in Toekalu in the Pacific. Availability of better bathymetry data, particularly near the coastline, can be used to further improve the model and thus the collection of such data should be a priority for the Maldives as it will have clear and direct benefits for risk management across the archipelago.

In addition to bathymetry data, the model friction parameter also has an influence on predictions of tsunami behaviour. Dilmen et al. (2018) studied the impact of different Manning coefficients in tsunami modelling within a reef environment at Tutuila island in American Samoa, and found that use of a single Manning's n value, as used in this study, was not sufficient to fully account for tsunami-induced flow within a reef environment. Further, Gelfenbaum et al. (2011), predict that beyond a critical reef width, the tsunami amplitude is dominated by the friction parameter, which generally reduces the tsunami amplitude. The availability of data to better describe the friction parameters is needed to facilitate model calibration.

Additionally, the model was run in a UTM (Universal Transverse Mercator) coordinate system, which introduces geometrical errors. However, comparison of the simulation results carried out in section 3.1.2, shows good agreement with field observations. This justifies its use here, especially in light of the other error sources listed above.



Lastly, parameters used in fault models have also been suggested to contribute to overall limitations in tsunami modelling (Poisson et al., 2011). We note that the numerical model used within this work, Thetis, has an adjoint model available. Similar studies for other natural hazards have utilised adjoint methods to perform more complete sensitivity analysis and uncertainty quantification, e.g. Warder et al. (2021). Such methods could be utilised for tsunami hazard assessment to quantify model
450 uncertainties arising from a variety of sources.

5 Conclusions

Detailed high-fidelity tsunami modelling of the Maldives archipelago has been conducted for the first time using a high-resolution bathymetry dataset, with a focus on nearshore maximum tsunami amplitudes. Modelled results, validated against field data obtained for the 2004 tsunami event, show that the model compares well with observational data. Model results
455 emphasize that tsunami risk assessments for the archipelago need to incorporate high-resolution modelling because Atoll shapes and island geography induce a high level of control over, and thus variability in the resulting tsunami amplitudes due to the development of complex refraction and reflection wave patterns.

On account of the large-scale coastal modifications seen across the Maldives archipelago in recent years (DNP, 2019), future work will need to take into account the possible impact of such large-scale modifications on the natural resilience of the islands
460 to minimize the impact of far-field tsunamis, as opposed to potentially exacerbating any localised risk. Coastal modifications have already been shown to affect bed stress (Rasheed et al., 2021) across the larger atoll domain as well as at the near shore regions of islands, and the results of this study could be incorporated in such future studies to better understand the resilience of islands to such events.

Code availability.

465 The source code of *Thetis* coastal ocean model used in this study is available from <https://thetisproject.org/> as well as <https://github.com/thetisproject/thetis>.

Data availability.

The data presented in this study can be viewed using the Atoll Tsunami Explorer App, available from <https://zubba1989.users.earthengine> as well as within the I-Hex (<https://i-hex.github.io/>) platform.

470 *Author contributions.* S



R ran the simulations, carried out the analysis of results and initiated the writing of the paper. SCW provided support for model setup and analysis of the results. MDP and YP provided supervision, guidance and insights at every stage of the project. All authors participated in the writing and editing of the paper.

Competing interests.

475 The authors declare that they have no conflict of interest.

Acknowledgements. The authors would like to acknowledge funding from a Research England GCRF award made to Imperial College London, and the Imperial College London Strategic Priorities Fund 2020-21 awarded for the Island Health Explorer project. SR would like to acknowledge PhD funding from the Islamic Development Bank and Imperial College London.



References

- 480 ADB: Multi Hazard risk atlas of the Maldives, Tech. rep., Asian Development Bank, <https://doi.org/http://dx.doi.org/10.22617/TCS200049>,
2020.
- Angeloudis, A., Kramer, S. C., Avdis, A., and Piggott, M. D.: Optimising tidal range power plant operation, *Applied Energy*, 212, 680–690,
2018.
- Areas, G. A.: GADM Database of Global Administrative Areas, version 2.8. 2015, URL <http://www.gadm.org>, 2018.
- 485 Avdis, A., Jacobs, T. C., Mouradian, L. S., Hill, J., and Piggott, D. M.: Meshing ocean domains for coastal engineering applications, in: The
European Community on Computational Methods in Applied Sciences and Engineering (ECCOMAS) VII Congress Proceedings, Crete,
Greece, June 5e10, 2016.
- Avdis, A., Candy, A. S., Hill, J., Kramer, S. C., and Piggott, M. D.: Efficient unstructured mesh generation for marine renewable energy
applications, *Renewable Energy*, 116, 842–856, <https://doi.org/10.1016/j.renene.2017.09.058>, <https://doi.org/10.1016/j.renene.2017.09.058>,
490 058, 2018.
- Baba, T., Mleczko, R., Burbidge, D., Cummins, P. R., and Thio, H. K.: The effect of the Great Barrier Reef on the propagation of the 2007
Solomon Islands tsunami recorded in northeastern Australia, in: *Tsunami Science Four Years after the 2004 Indian Ocean Tsunami*, pp.
2003–2018, Springer, 2008.
- Betzler, C., Lindhorst, S., Lüdmann, T., Weiß, B., Wunsch, M., and Braga, J. C.: Grain size distribution of the lagoonal deposits within
495 the South Malé Atoll, Maldives, Indian Ocean, <https://doi.org/10.1594/PANGAEA.858886>, <https://doi.org/10.1594/PANGAEA.858886>,
supplement to: Betzler, C et al. (2015): The leaking bucket of a Maldives atoll: Implications for the understanding of carbonate platform
drowning. *Marine Geology*, 366, 16–33, <https://doi.org/10.1016/j.margeo.2015.04.009>, 2016.
- Byrne, D. E., Sykes, L. R., and Davis, D. M.: Great thrust earthquakes and aseismic slip along the plate boundary of the Makran subduction
zone, *Journal of Geophysical Research: Solid Earth*, 97, 449–478, 1992.
- 500 Dilmen, D. I., Roe, G. H., Wei, Y., and Titov, V. V.: The role of near-shore bathymetry during tsunami inundation in a reef island setting: A
case study of Tutuila Island, *Pure and Applied Geophysics*, 175, 1239–1256, 2018.
- DNP: Statistical Year Book of Maldives 2019, <http://statisticsmaldives.gov.mv/yearbook/2019/>, 2019.
- Duvat, V. K. and Magnan, A. K.: Rapid human-driven undermining of atoll island capacity to adjust to ocean climate-related pressures,
Scientific reports, 9, 1–16, 2019.
- 505 Emerton, L., Baig, S., and Saleem, M.: Valuing biodiversity: the economic case for biodiversity conservation in the Maldives, AEC Project,
Ministry of Housing, Transport and Environment, Maldives, 2009.
- Ford, M., Becker, J. M., Merrifield, M. A., and Song, Y. T.: Marshall Islands fringing reef and atoll lagoon observations of the Tohoku
tsunami, *Pure and Applied Geophysics*, 171, 3351–3363, 2014.
- Fritz, H. M., Synolakis, C. E., and McAdoo, B. G.: Maldives field survey after the December 2004 Indian Ocean tsunami, *Earthquake Spectra*,
510 22, 137–154, 2006.
- Fujima, K., Shigihara, Y., Tomita, T., Honda, K., Nobuoka, H., Hanzawa, M., Fujii, H., Ohtani, H., Orishimo, S., Tatsumi, M., et al.: Survey
results of the Indian Ocean tsunami in the Maldives, *Coastal Engineering Journal*, 48, 81–97, 2006.
- Gardiner, J. S.: The formation of the Maldives, *The Geographical Journal*, 19, 277–296, <https://www.jstor.org/stable/1775312>, 1902.
- Gardiner, J. S.: The Fauna and Geography of the Maldive and Laccadive Archipelagoes: Being the Account of the Work Carried on and of
515 the Collections Made by an Expedition During the Years 1899 and 1900, vol. 1, University press, 1903.



- Gelfenbaum, G., Aposos, A., Stevens, A. W., and Jaffe, B.: Effects of fringing reefs on tsunami inundation: American Samoa, *Earth-Science Reviews*, 107, 12–22, 2011.
- Gica, E.: A tsunami forecast model for Midway Atoll, 2015.
- Gorelick, N., Hancher, M., Dixon, M., Ilyushchenko, S., Thau, D., and Moore, R.: Google Earth Engine: Planetary-scale geospatial analysis for everyone, *Remote sensing of Environment*, 202, 18–27, 2017.
- 520 Grilli, S. T., Ioualalen, M., Asavanant, J., Shi, F., Kirby, J. T., and Watts, P.: Source constraints and model simulation of the December 26, 2004, Indian Ocean Tsunami, *Journal of Waterway, Port, Coastal, and Ocean Engineering*, 133, 414–428, 2007.
- Harig, S., Pranowo, W. S., Behrens, J., et al.: Tsunami simulations on several scales, *Ocean Dynamics*, 58, 429–440, 2008.
- Hass, H.: Expedition into the unknown: a report on the expedition of the research ship Xarifa to the Maldives and the Nicobar Islands and on a series of 26 television films, Hutchinson, 1965.
- 525 Hmadhoon Hameed: TSUNAMI IMPACT ASSESSMENT 2005 REPUBLIC OF MALDIVES: A socio-economic countrywide assessment at household level, six months after the tsunami, Tech. rep., Government of Maldives, https://maldivesindependent.com/files/2015/03/TIA_2005_Main_Report-UNDP-and-Nat.-Planning-Detp.pdf, 2005.
- Kan, H., Ali, M., and Riyaz, M.: The 2004 Indian Ocean tsunami in the Maldives: scale of the disaster and topographic effects on atoll reefs and islands, National Museum of Natural History, Smithsonian Institution, 2007.
- 530 Kärnä, T., De Brye, B., Gourgue, O., Lambrechts, J., Comblen, R., Legat, V., and Deleersnijder, E.: A fully implicit wetting–drying method for DG-FEM shallow water models, with an application to the Scheldt Estuary, *Computer Methods in Applied Mechanics and Engineering*, 200, 509–524, 2011.
- Kärnä, T., Kramer, S. C., Mitchell, L., Ham, D. A., Piggott, M. D., and Baptista, A. M.: Thetis coastal ocean model: Discontinuous Galerkin discretization for the three-dimensional hydrostatic equations, *Geoscientific Model Development*, 11, 4359–4382, <https://doi.org/10.5194/gmd-11-4359-2018>, 2018.
- 535 Kench, P. S., McLean, R. F., Brander, R. W., Nichol, S. L., Smithers, S. G., Ford, M. R., Parnell, K. E., and Aslam, M.: Geological effects of tsunami on mid-ocean atoll islands: The Maldives before and after the Sumatran tsunami, *Geology*, 34, 177–180, 2006.
- Kraines, S., Yanagi, T., Isobe, M., and Komiyama, H.: Wind-wave driven circulation on the coral reef at Bora Bay, Miyako Island, *Coral reefs*, 17, 133–143, 1998.
- 540 Luthfee, M. I.: Dhivehi Raajjeige Geographyge’ Vanavaru, vol. 1,2, Ministry of Education, 1995.
- Naseer, A. and Hatcher, B. G.: Inventory of the Maldives’ coral reefs using morphometrics generated from Landsat ETM+ imagery, *Coral Reefs*, 23, 161–168, 2004.
- Naseer, A. et al.: Pre-and post-tsunami coastal planning and land-use policies and issues in the Maldives, in: Proceedings of the workshop on coastal area planning and management in Asian tsunami-affected countries, pp. 27–29, FAO Bangkok, 2006.
- 545 Okada, Y.: Internal deformation due to shear and tensile faults in a half-space, *Bulletin of the seismological society of America*, 82, 1018–1040, 1992.
- Okal, E. A. and Synolakis, C. E.: Far-field tsunami hazard from mega-thrust earthquakes in the Indian Ocean, *Geophysical journal international*, 172, 995–1015, 2008.
- 550 Orpin, A. R., Rickard, G. J., Gerring, P. K., and Lamarche, G.: Tsunami hazard potential for the equatorial southwestern Pacific atolls of Tokelau from scenario-based simulations, *Natural Hazards and Earth System Sciences*, 16, 1239–1257, 2016.



- Pan, W., Kramer, S. C., and Piggott, M. D.: Multi-layer non-hydrostatic free surface modelling using the discontinuous Galerkin method, *Ocean Modelling*, 134, 68 – 83, <https://doi.org/https://doi.org/10.1016/j.ocemod.2019.01.003>, <http://www.sciencedirect.com/science/article/pii/S1463500318302312>, 2019.
- 555 Poisson, B., Oliveros, C., and Pedreros, R.: Is there a best source model of the Sumatra 2004 earthquake for simulating the consecutive tsunami?, *Geophysical Journal International*, 185, 1365–1378, 2011.
- Rasheed, S., Warder, S. C., Plancherel, Y., and Piggott, M. D.: An Improved Gridded Bathymetric Dataset and Tidal Model for the Maldives Archipelago, *Earth and Space Science*, p. e2020EA001207, 2020.
- Rasheed, S., Warder, S. C., Plancherel, Y., and Piggott, M. D.: Response of tidal flow regime and sediment transport in North Malé Atoll, Maldives, to coastal modification and sea level rise, *Ocean Science*, 17, 319–334, 2021.
- 560 Rathgeber, F., Ham, D. A., Mitchell, L., Lange, M., Luporini, F., Mcrae, A. T. T., Bercea, G.-T., Markall, G. R., and Kelly, P. H. J.: Firedrake: Automating the Finite Element Method by Composing Abstractions, *ACM Trans. Math. Softw.*, 43, <https://doi.org/10.1145/2998441>, <https://doi.org/10.1145/2998441>, 2016.
- Riyaz, M. and Suppasri, A.: Geological and Geomorphological Tsunami Hazard Analysis for the Maldives Using an Integrated WE Method and a LR Model, *Journal of Earthquake and Tsunami*, 10, 1650 003, 2016.
- 565 Riyaz, M., Park, K.-H., Ali, M., and Kan, H.: Influence of geological setting of islands and significance of reefs for tsunami wave impact on the Atoll Islands, Maldives, *Bulletin of engineering geology and the environment*, 69, 443–454, 2010.
- RMSI: Developing a Disaster Risk Profile for Maldives, Tech. rep., United Nations Development Programme, <http://files.epa.gov.mv/file/1522>, 2006.
- 570 Rosman, J. H. and Hench, J. L.: A framework for understanding drag parameterizations for coral reefs, *Journal of Geophysical Research: Oceans*, 116, 2011.
- Sewell, R. S.: An account of Addu Atoll, British Museum, 1936.
- Spalding, M., Spalding, M. D., Ravilious, C., Green, E. P., et al.: World atlas of coral reefs, Univ of California Press, 2001.
- Stoddart, D. R.: Reef studies at Addu Atoll, Maldives: preliminary results of an expedition to Addu Atoll in 1964, Pacific Science Board, National Academy of Sciences–National Research Council, 1966.
- 575 Synolakis, C. E. and Bernard, E. N.: Tsunami science before and beyond Boxing Day 2004, *Philosophical Transactions of the Royal Society A: Mathematical, Physical and Engineering Sciences*, 364, 2231–2265, 2006.
- Tanioka, Y., Kususe, T., Kathioli, S., Nishimura, Y., Iwasaki, S.-I., Satake, K., et al.: Rupture process of the 2004 great Sumatra-Andaman earthquake estimated from tsunami waveforms, *Earth, planets and space*, 58, 203–209, 2006.
- 580 Tonini, R., Armigliato, A., Pagnoni, G., and Tinti, S.: Modeling the 2004 Sumatra tsunami at Seychelles Islands: site-effect analysis and comparison with observations, *Natural hazards*, 70, 1507–1525, 2014.
- Wadey, M., Brown, S., Nicholls, R. J., and Haigh, I.: Coastal flooding in the Maldives: an assessment of historic events and their implications, *Natural Hazards*, 89, 131–159, 2017.
- Warder, S. C., Horsburgh, K. J., and Piggott, M. D.: Adjoint-based sensitivity analysis for a numerical storm surge model, *Ocean Modelling*, 585 160, 101 766, 2021.
- Weatherall, P., Marks, K. M., Jakobsson, M., Schmitt, T., Tani, S., Arndt, J. E., Rovere, M., Chayes, D., Ferrini, V., and Wigley, R.: A new digital bathymetric model of the world’s oceans, *Earth and Space Science*, 2, 331–345, 2015.
- Wessel, P. and Smith, W.: GSHHG—A Global Self-Consistent, Hierarchical, High-Resolution Geography Database, Honolulu, Hawaii, Silver Spring, Maryland.(URL: <http://www.soest.hawaii.edu/pwessel/gshhg/>(accessed 10 January 2013), 2013.



- 590 Wijetunge, J.: Nearshore tsunami amplitudes off Sri Lanka due to probable worst-case seismic scenarios in the Indian Ocean, Coastal Engineering, 64, 47–56, 2012.
- World Bank, A. D. B. and System, U.: Maldives Tsunami: Impact and Recovery, Joint Needs Assessment, 2005.